

Spectroscopic Study of Interactions Between Model Direct Dyes and Cotton

Anna Pielesz

Faculty of Textile Engineering and Environmental Protection, Institute of Textile Engineering and Polymer Materials, University of Bielsko-Biala, Bielsko-Biala, Poland

Received 1 May 2006; accepted 17 August 2006

DOI 10.1002/app.25566

Published online in Wiley InterScience (www.interscience.wiley.com).

ABSTRACT: Although examined for years, interactions between direct dyes and the chemical structure of cotton cellulose remain an interesting, and still not entirely known, chemical phenomenon occurring in the fiber. Ten model azo dyes have been studied in aqueous solution, as dye powders and on cotton fabric using ^{13}C MAS NMR and UV-visible spectroscopy. NMR spectroscopy indicates that model azo dyes, especially dye 8, interact by π -stacking at the central biphenyl

group, and that there is hydrogen bonding with cellulose. Model azo dyes are present as the azo or hydrazone tautomer. The UV-visible λ_{max} indicate that shifts are attributed to adsorption of model azo dyes into cellulose surfaces. © 2007 Wiley Periodicals, Inc. *J Appl Polym Sci* 104: 758–766, 2007

Key words: NMR; UV-visible; dyes/pigments; cotton fibers; microstructure

INTRODUCTION

Cotton is a hydrophilic natural cellulose fiber whose porous structure facilitates the penetration of various solutes, including organic dyes. As a cellulose-based polymer, it consists of D-glucose units joined by β -1,4-glycosidic linkages, and it is well known that the cellulose chains associate with one another via intermolecular hydrogen bonds. The resultant system of polymer chains coalesces to form microfibrils that are organized into macrofibrils and subsequently into fibers, Lewin and Pearse.¹ In the solid state, it has at least four distinct polymorphic forms, the most common of which are called cellulose I and cellulose II, Bikales and Segal.²

Based on results from ^{13}C MAS NMR spectroscopy on several native cellulose materials, Van der Hart et al. discovered (Atalla and VanderHart,³ VanderHart and Atalla^{4,5}) that the ordered region of native cellulose is a mixture of two crystalline modifications, cellulose I_{α} and cellulose I_{β} . Cellulose I_{α} is believed to be the dominant form in bacterial and algal cellulose, while cellulose I_{β} predominates in higher plants such as cotton and ramie (Atalla and VanderHart,³ VanderHart and Atalla^{4,5}). The ^{13}C MAS NMR spectrum of pure cellulose is characteristic of a completely amorphous material, Atalla et al.,⁶ and shows four well-separated peaks, which can be attributed to the corresponding structural elements, Radloff et al.⁷: 104.6 ppm, C_1 ; 83.9 ppm, C_4 ; 74.5 ppm, $\text{C}_{2,3,5}$; 62.2 ppm, C_6 . Other

authors, Sun et al.,⁸ Love et al.⁹ describe these chemical shifts in a slightly different way, distinguishing, Adebajo and Frost¹⁰: 105.3 ppm (C_1 of cellulose); 89.5 ppm (C_4 of crystal cellulose); 83.2 ppm (C_4 of amorphous cellulose); 74.7 ppm ($\text{C}_{2, 3, 5}$ linked polysaccharides) and 62.1 ppm (C_6 of crystal-surface cellulose).

NMR spectroscopy is typically used for separate analyses of dyes (Viscardi et al.,¹¹ Wiench et al.,¹² Voss,¹³ Lyčka et al.¹⁴), dyes solutions, Abbott et al.¹⁵ or cotton, textiles or modified polymers based on cellulose mixtures, (Hirai et al.,¹⁶ Colletti and Mathias,¹⁷ Princi et al.,¹⁸ Chanzy et al.,¹⁹ Larsson et al.,²⁰ Dudley et al.,²¹ Lennholm et al.,²² Randloff et al.,⁷ Adebajo and Frost¹⁰).

Spectroscopic studies of the intermolecular interactions of azo dyes in solution and in cellulose were described (Abbott et al.,¹⁵ Abbott et al.,²³ Batchelor and Oakes,²⁴ Abbott et al.,^{25–27} Yamaki et al.²⁸). They report NMR, resonance Raman, IR, and UV-visible spectroscopic studies of dyes in solution and in cellulose. For example, NMR spectra from solution samples provide information on tautomer forms, hydrogen bonding, and deuterium exchange, Abbott et al.¹⁵

The crystal structure of the native cellulose has been continuously investigated by solid-state NMR spectroscopic analysis. But, there have been few attempts to explain how dyes interact with cellulose.

EXPERIMENTAL

The model direct dyes were synthesized at North Carolina State University at Raleigh, USA, Bae and Freeman.²⁹ A 1% dyeing (owf) was carried out under neutral conditions at a 60 : 1 liquor ratio. A sample of cot-

Correspondence to: A. Pielesz (apielesz@ath.bielsko.pl).

ton fabric (0.5 g) was wetted out with hot water and added to a dyebath (30 mL) at 60°C. The bath temperature was raised to 95°C and held there for 30 min. After adding Na₂SO₄ (0.05 g), dyeing was continued for 30 min. The dyed fabric was then rinsed with cold water and air-dried.

The cotton samples were also treated with acidic and alkaline artificial sweat, its contents defined by the "Textiles – Tests for color fastness – Part E04: Color fastness to perspiration" standard.

Cotton samples were also treated with old, thermal, and effort artificial sweats, Gudewill.³⁰

The samples of cotton, dyed cotton fabric and dye powders were examined with a Bruker 400 MHz spectrometer. The samples were centrifuged at 8 kHz.

Spectra of dyes aqueous solutions (10⁻⁵ mol L⁻¹ aqueous solutions of the dye) and dyed cotton fabric were taken using a UV–Vis spectrophotometer, model U-2001 HITACHI with the following parameters: range 300–800nm, scanning rate 100 nm/min.

The structures of the model dyes are presented in Figure 1.

RESULTS AND DISCUSSION

Azo dyes, in general, are well known to form dimers or higher aggregates at high concentration in solution,

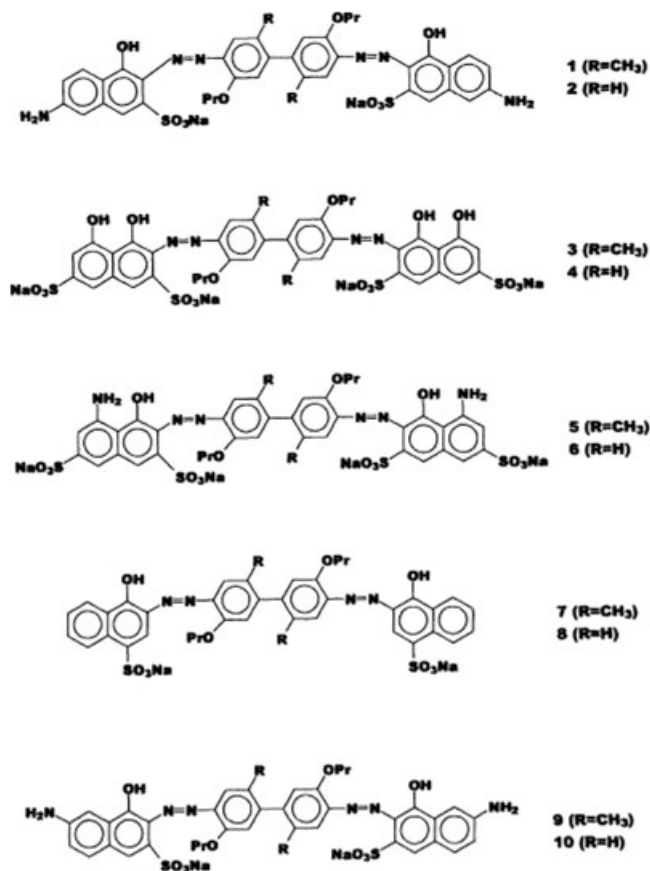


Figure 1 Structure of the dyes selected for examination.

Murakamei,³¹ because of the presence of dye–dye intermolecular interactions.

Direct dyeing is a complicated and very little understood process, although it seems very simple in terms of applications.

Direct dyes aggregate to larger compounds. Aggregation is promoted by a high ratio of relative molecular mass to ionic group content, Shore.³² The direct dyes aggregate more readily than most of the other classes of water-soluble dyes. Solutions contain a mixture of aggregates of various sizes in dynamic equilibrium. Individual ions, dimers, or trimers are removed by adsorption onto the fiber surface during dyeing, and larger aggregates break down to maintain a similar overall distribution of aggregate sizes. The extent of aggregation of a direct dye decreases with increasing temperature and increases with increasing concentration of added electrolyte or of the dye itself. The degree of aggregation is often negligible under normal dyeing conditions at the boil even in the presence of an electrolyte, Shore.³²

The relative tendencies to aggregate depend on different dye structures. For example, under given conditions of temperature and electrolyte concentration, model direct dye 8 (Fig. 1) is much more highly aggregated than other dyes 1, 2, 3, 4, 7 (Fig. 1). Perhaps dye 8 aggregates more because it has fewer SO₃ groups, and these are arranged in such a way that the planar central region of the molecule is subject to less steric bulk than in the other dyes.

All of the dyes are disulphonated disazo dyes, but presumably the two phenolic groups and the hydrogen in dye 8 provide much greater scope for intermolecular hydrogen bonding.

In particular, it is important to understand the structural factors that determine the nature of dye–dye intermolecular interactions, and how they may be affected by interactions with the molecular surfaces of cellulose, Abbott et al.²³ Cellulose provides a microporous medium consisting of polysaccharide chains arranged into crystalline and amorphous regions with pores of ~ 1–3 nm dimension where binding occurs, Krässig.³³ However, relatively little is known about the structure of the amorphous phase or the behavior of the cellulose molecules with the nanopores, Frantz et al.³⁴

But, in contrast to the wool fiber, cellulose does not contain ionic sites, and as such is not able to fix dyes through respective Coulomb forces.

As a consequence, direct dyeing of cotton requires specific structural features of the dye molecules, resulting in an overall affinity for the cellulose fiber that is called substantivity, Schüürmann and Funar-Timofei.³⁵

One of the parameters that examine the substantivity is the degree of dyes exhaustion E_k .

Our experiments, Pieliesz et al.³⁶ indicate that the degree of dyes exhaustion is $E_k = 69\%$ for the cotton

TABLE I
Assignments for ^{13}C MAS NMR Chemical Shifts

Sample	Chemical shifts (ppm)						
	C_1	C_1 amorph	C_4	C_4 amorph=surf	$\text{C}_{2, 3, 5}$	C_6	C_6 surf
SB	105.4	104.6	88.7	83.9	74.7; 71.7	65.1	62.1
1B	105.6	104.2	88.8	83.9	74.9; 72.2; 71.5	65.1	62.1
2B	105.1	104.2	88.7	83.7	74.8; 71.5	65.2	62.1
3B	106.2	104.9	89.4	84.6	75.5; 72.9; 72.2	65.8	63.0
4B	106.2	104.9	89.4	84.9	75.5; 72.9; 72.2	65.8	63.6
7B	105.7	104.3	88.8	84.1	74.9; 72.2; 71.5	65.2	63
8B	106.8	105.2	89.9	85.1	75.9; 73.5; 72.4	66.1	63.9

SB, undyed cotton cellulose; 1B, 2B, 3B, 4B, 7B, 8B: cotton cellulose dyed with dye 1,2,3,4,7,8.

dyed with dye 8, and it is greater than the value for the remaining dyes. It means about a successful uptake from aqueous solution and stable fixation of model dye 8 in the cotton fiber.

To analyze the interactions between model direct dyes and cotton cellulose, raw, undyed cotton fabric was compared with its dyed equivalents. Table I shows the basic values of chemical shifts for cotton and the dyes selected (if the values obtained for the latter occur in the region of band interference).

At first look, it can be said that the spectra of dyed cotton and raw cotton in Figure 2 and Table I do not differ. One thing worth noting is the region attributed to the atoms of $\text{C}_{2, 3, 5}$, C_1 , and C_4 of polysaccharides. Here, all the selected model dyes also reveal more or less intense bands.

One of the reasons that makes the analysis of the solid-state NMR spectrum of the native cellulose confusing is that the native cellulose always appears as a composite of I_α and I_β allomorphs and noncrystalline regions, Atalla and VanderHart,³ VanderHart and Atalla.⁴ The completely pure I_α and I_β cellulose have not been obtained from any species of plants and animals. All native celluloses contain crystalline and noncrystalline phases, Atalla and VanderHart,³⁷ and the structure of cellulose microfibrils is not well understood at the molecular level and is still the subject of controversy, Sakellariou et al.,³⁸ Lasage et al.³⁹ CP/MAS ^{13}C NMR spectra of *Cladophora* cellulose (I_α -rich) and that of cellulose after the annealing treatment (I_β -rich) are, respectively, the almost pure I_α and I_β celluloses, Komo et al.⁴⁰

For the assignment of the ^{13}C signal of cellulose in the solid state, Bardet et al.⁴¹ applied 2D NMR technique to ^{13}C -enriched wood chips from aspen grown under a 20% $^{13}\text{CO}_2$ atmosphere and observed the two broad signals around 76 and 74 ppm in the region of signals corresponding to C_2 , C_3 , and C_5 .

The same signals, especially for cotton dyed with model dye 8 (75.9 and 72.4 ppm) and model dyes 3 and 4 (75.5 and 72.2 ppm) were observed (Table I and Fig. 2).

The ^{13}C NMR behavior of C_4 in cellulose is particularly divergent from theoretical predictions, Koch et al.,⁴² Wilson et al.⁴³ Differences in the chemical environment of C_4 must be due to noncovalent effect, either intramolecular (conformation) or intermolecular (chain packing, which in cellulose means intermolecular hydrogen bonding), Vi tor et al.⁴⁴ Intermolec-

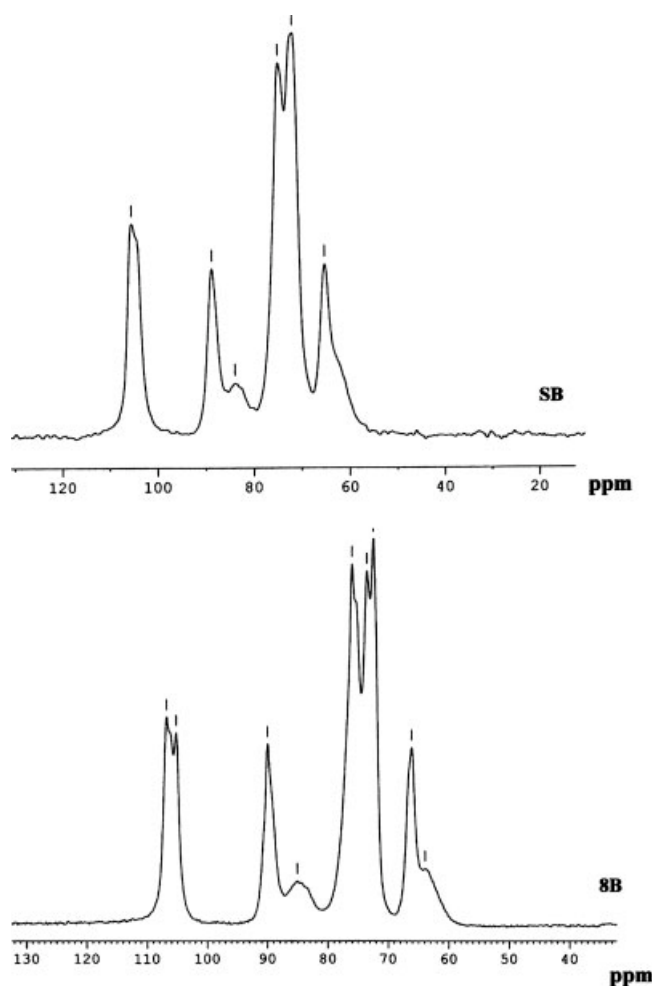


Figure 2 ^{13}C MAS NMR spectra of: (a) undyed cotton cellulose-SB; (b) cotton cellulose dyed with dye 8-8B.

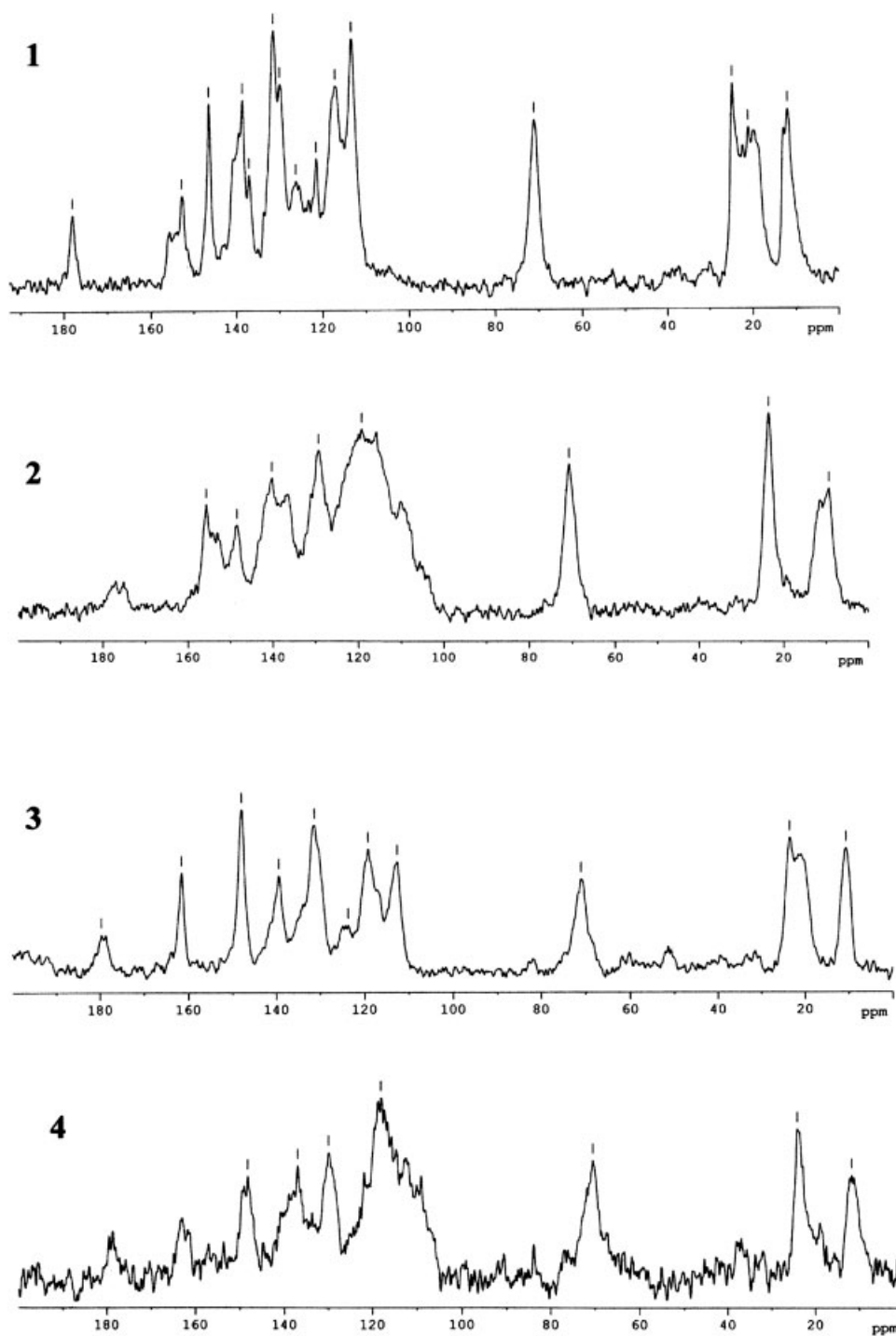


Figure 3 ^{13}C MAS NMR spectra of 10 model direct dyes.

ular hydrogen bonding could affect the C_4 chemical shift indirectly by locking the rotation of O_2 , O_3 , or C_6 and altering their stereoelectronic interactions with C_4 , Viëtor et al.⁴⁴

When comparing undyed and dyed (with model dyes 3, 4 and 8) cotton, one should note the changes within chemical shift around C_4 and C_6 (for example 66.1 ppm for the cotton dyed with dye 8) (Table I). The biggest changes can be observed around C_4

described as amorphous, Larson et al.²⁰ or C_4 of crystal-surface cellulose, Love et al.⁹ In particular, using dye 8 results in a substantial change of the chemical shift value (Table I).

Azo dyes in which the azo group is conjugated with a hydroxyl group can exhibit azo-hydrazone tautomerism, Lyčka et al.⁴⁵ Dyes that occur as the azo tautomer show a ^{13}C NMR resonance at ~ 156 ppm from carbon attached to the hydroxyl group, whereas those

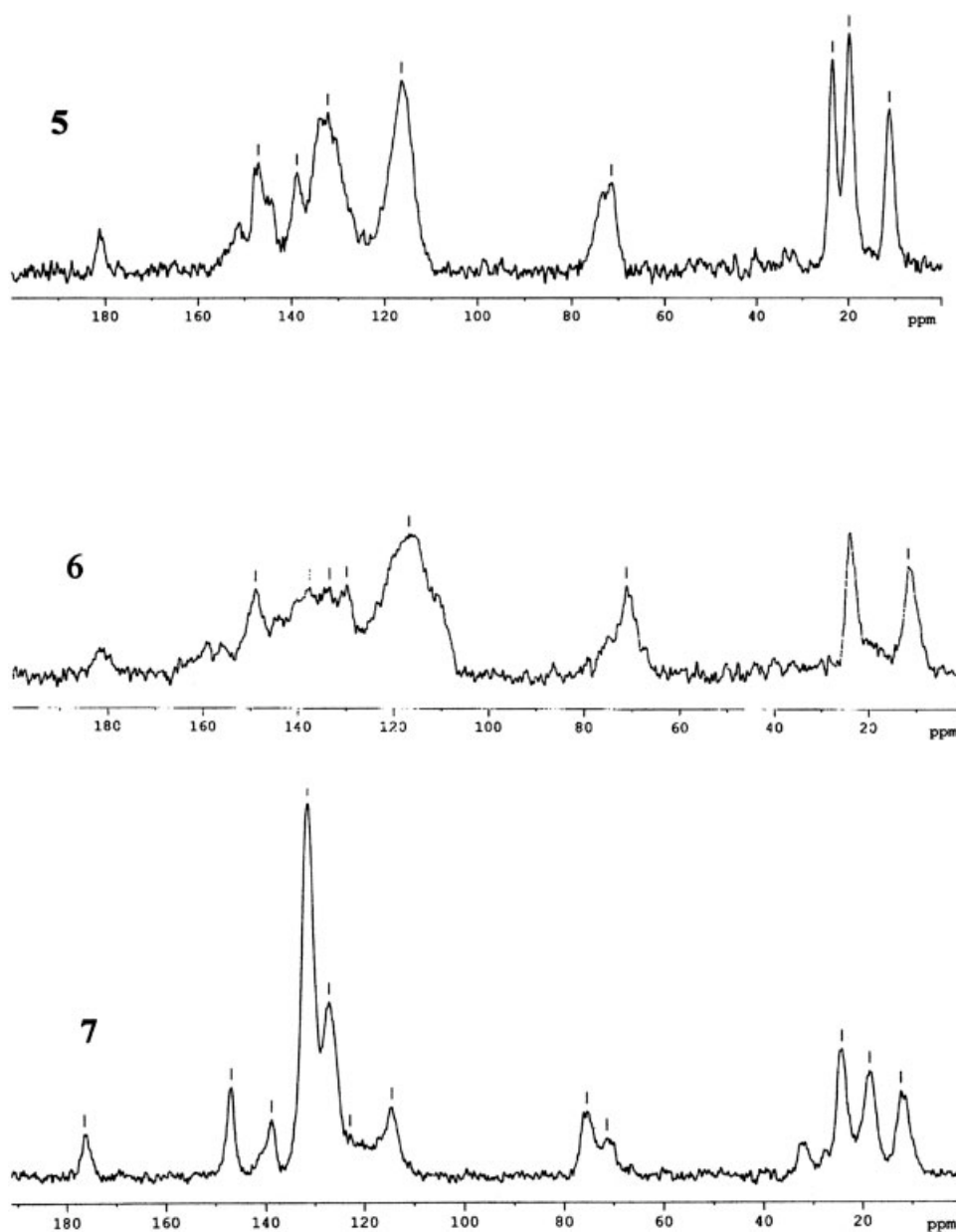


Figure 3 (Continued from the previous page)

that occur as the hydrazone tautomer show a resonance at ~ 180 ppm for the same carbon atom within a carbonyl group. Dyes that occur as both tautomers show a single resonance between these limits, because of rapid tautomerisation, with the position determined by the relative concentration of the two tautomers, Cross et al.⁴⁶ The ^{13}C NMR and ^1H NMR spectra of the two tautomers from DMF, DMSO, and D_2O samples of Direct Blue 1 are presented by Abbott et al.^{15,23}

The ^{13}C MAS NMR spectra of 10 model dyes complement, a full spectral characteristic of model direct dyes are presented (Fig. 3 and Table II).

We recently reported IR and resonance Raman spectroscopic studies of the model direct dyes in the

microporous cellulose environments of cotton, Pielez et al.^{47,48} The studies revealed aspects of the intramolecular hydrogen-bonding interactions with the monomer (probably a hydrazone tautomer in the environments) and of the intermolecular interactions between the monomer and cellulose molecules.

The article, Pielez et al.⁴⁸ attempts to provide a general answer to the question of how model direct dyes interact with the structure of cellulose. For assessing the interactions between model direct dyes and cotton cellulose, the 1D FTR and 2D FTR were chosen. To this end, synchronic and asynchronous 2D maps for FTR spectra were constructed. In a synchronic map, bands with 1100 cm^{-1} and 1125 cm^{-1} wave numbers are responsible for the interaction of

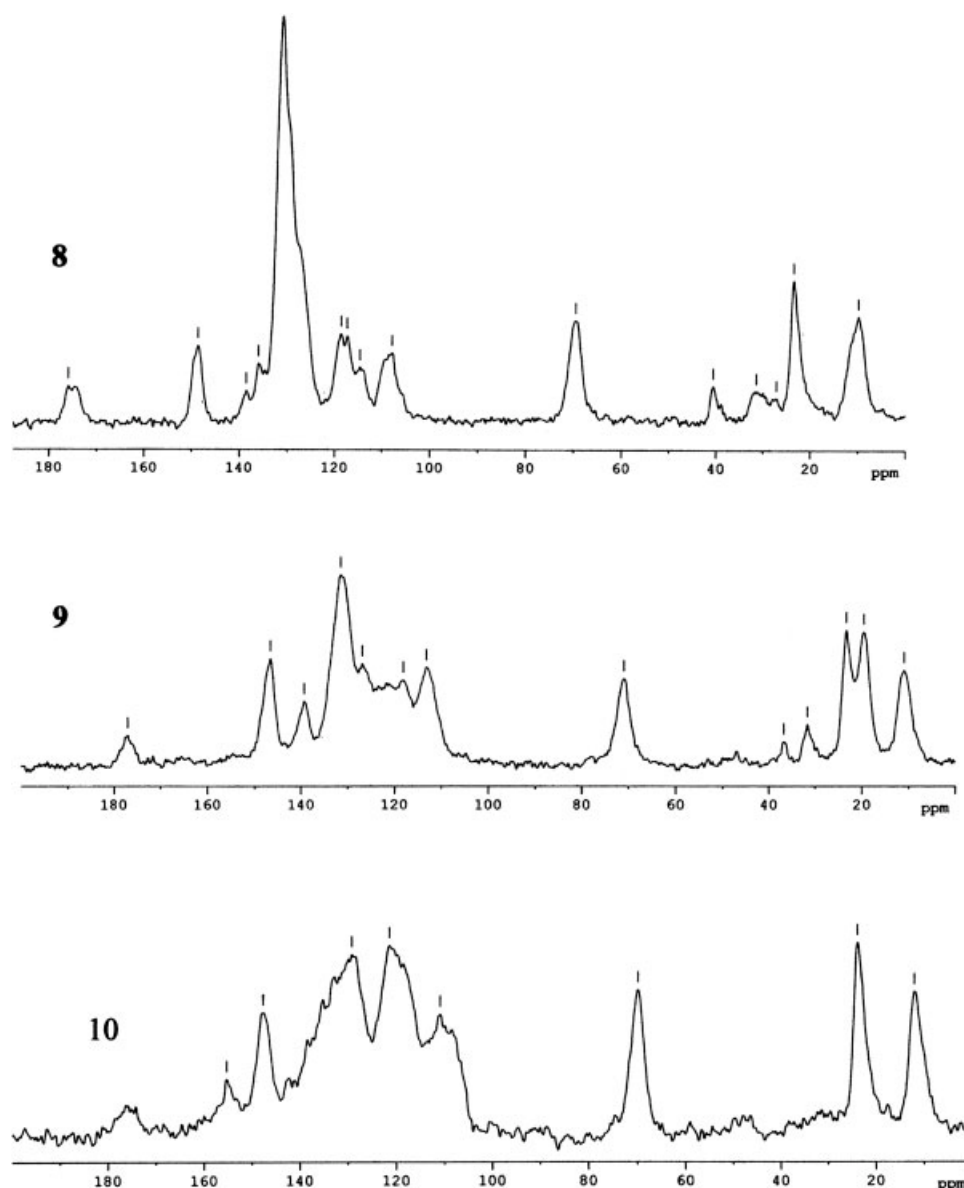


Figure 3 (Continued from the previous page)

model dyes with COC groups or CC rings (at 1125 cm^{-1}) in cotton. Information obtained through analyzing synchronic maps is confirmed by the analysis of bands generated in asynchronous maps.

The article, Pieleesz et al.⁴⁷ pertains to the use of FT-Raman spectroscopy to determine the places at which model direct dyes interact with cotton-cellulose. In addition to finding direct dye-cellulose interactions involving hydroxyl groups in the host fiber, it is postulated that intermolecular interactions exist between dye molecules and glycosidic groups. The usefulness of the conventional FTIR spectroscopy for analyzing dyed cotton has been shown, and results from this method are compared with data from the more popular DRIFT method.

TABLE II
 ^{13}C NMR Chemical Shifts (ppm) of Same
Model Azo Dyes

Dye	Chemical shifts (ppm)
1	177.9, -, 70.9
2	176.5, 155.8, 70.8
3	179.7, -, 70.9
4	176.4, -, 70.4
5	179.9, -, 71.4
6	179.8, -, 71.2
7	176.4, -, 75.3; 71.3
8	175.9, -, 69.5
9	177.0, -, 70.9
10	176.4, 155.3, 69.8

1–10, azo dyes.

TABLE III
UV-Visible Absorption Band Position of 10 Model Azo Dyes in Aqueous Solution and Cotton and Cotton Dyed and Treated with Artificial Sweats

Dye	λ_{\max} for aqueous dye solution and λ_{\max} for dyed cotton fabric sweats treatment						
	Dye (nm)	Cotton (nm)	Alkaline (nm)	Acidic (nm)	Old (nm)	Effort (nm)	Thermal (nm)
1	514	547	551	545	568	548	548
2	550	571	571	570	545	572	572
3	582	585	584	584	585	586	586
4	557	598	600	603	594	603	593
5	585	598	599	602	595	603	594
6	574	605	605	606	610	608	607
7	530	561	561	561	561	563	561
8	569	580	583	582	581	581	580
9	537	571	571	571	573	572	572
10	572	604	604	604	614	604	604

1–10, azo dyes.

The spectra in aqueous solutions show a strong visible bands (Table III, Figs. 4 and 5), which give the intense blue, purple, or violet color of the dyes, and a weaker UV bands at ~ 320 nm. The profile of the visible bands is sensitive to environment (for example in Figs. 6 and 7): in water solutions, the main peak is at ~ 514 nm with a shoulder at ~ 547 nm and in cotton, the peak occurs at 547 nm (Fig. 6). Also, for model dye 8 (Fig. 7) in water solutions, the main peak is at ~ 569 nm with a shoulder at ~ 658 nm, and in cotton, the peak occurs at 580 nm.

Cotton samples were also treated with artificial sweats. Measurements were taken for dyed cotton textiles as well as for a dyed textile that was subjected to the influence of various solutions of artificial sweats (alkaline, acidic, old sweat, thermal sweat, and effort sweat). The highest absorbance values, which do not change when fibers are treated with artificial sweats, were obtained for dyeing with model dye 8 (Fig. 7). The UV-visible spectrum of model dye 8 in cotton treated with artificial sweats showed no changes with different sweats pH. The red-shift in the absorption maximum of dye 8 observed on going from solution to cotton shows similar changes as in Abbott et al.²⁶ It

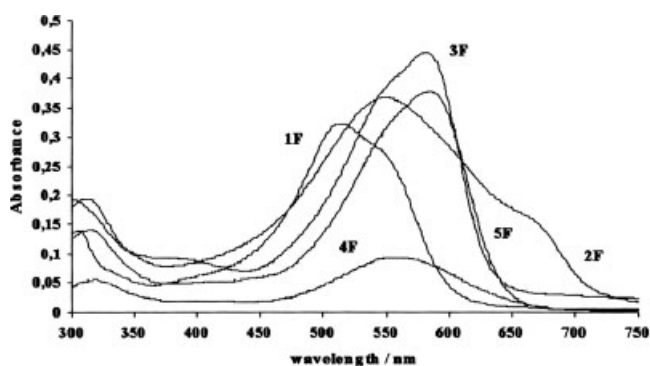


Figure 4 UV-visible spectra of model direct dyes: 1, 2, 3, 4, 5.

may be attributed to a change in the energy of either to ground and/or to the excited electronic state, probably arising from a small change in the structure of the dye on surface deposition, Abbott et al.²⁶ The general shift in the UV-visible band positions with medium can be interpreted in terms of increasing polarity from cotton ($\epsilon \approx 5$) to water ($\epsilon = 80$) that model dyes are more polar in the ground state than in the excited state, Abbott et al.²⁷

Other effect will also influence the UV-visible spectra of model dyes. For example, specific intermolecular interactions with the medium, including hydrogen-bonding (evidenced by FTIR and FTR spectra), Pielesz et al.^{47,48}

Other effect may include structural changes with the dyes that arise from surface adsorption, consistent with interpretation of the ^{13}C NMR data (Table I). This interpretation is consistent with the molecular structure of model dyes, the central biphenyl gives a characteristic red-shift on going from a twisted conformation in solution to a more planar form in the solid, Abbott et al.²³

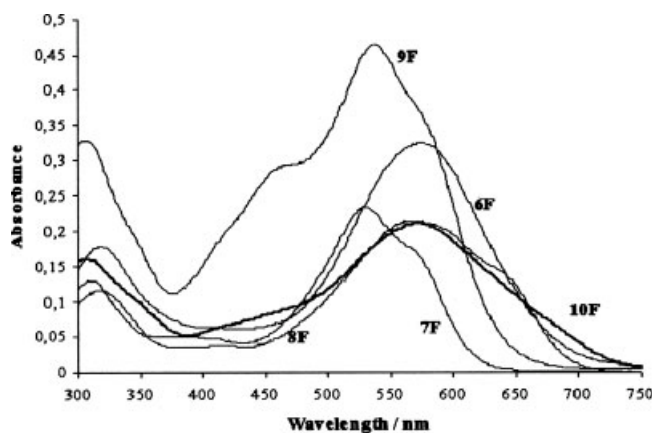


Figure 5 UV-visible spectra of model direct dyes: 6, 7, 8, 9, 10.

Analyzing the dye–cotton cellulose interactions is difficult. A combination of Raman, IR and UV–visible spectroscopies has been used earlier, (Pielesz et al.^{36,47,48}) to deduce the molecular interactions of model direct dyes in cotton cellulose.

CONCLUSIONS

In general, cotton cellulose may interact with a guest molecule in several ways, including specific dipole–dipole and hydrogen bonding interactions. All of the dyes possess an extended planar π -electron system, which is a determining factor for dye–fiber interaction via van der Waals forces. These dyes have sulfonic acid groups, which enhance their solubility in water; electrostatic interactions may also be relevant. From the spectroscopic point of view, model dyes are azo-dyes, with high absorptivity, which can undergo solvatochromic shifts depending on the dye–solvent interactions.

Issues for further discussion put forward in this work include a preliminary evaluation of the usefulness of ^{13}C MAS NMR spectroscopy for analyzing subtle structural changes in cotton cellulose. Since the process of dyeing cotton with direct dyes is usually explained as dye adsorption on fiber surface, such changes of the profile of ^{13}C MAS NMR spectra are hard to interpret in detail.

It seems that employing analyses of two-dimensional NMR spectra and advanced statistic processing may, in the future, help to explain better this phenom-

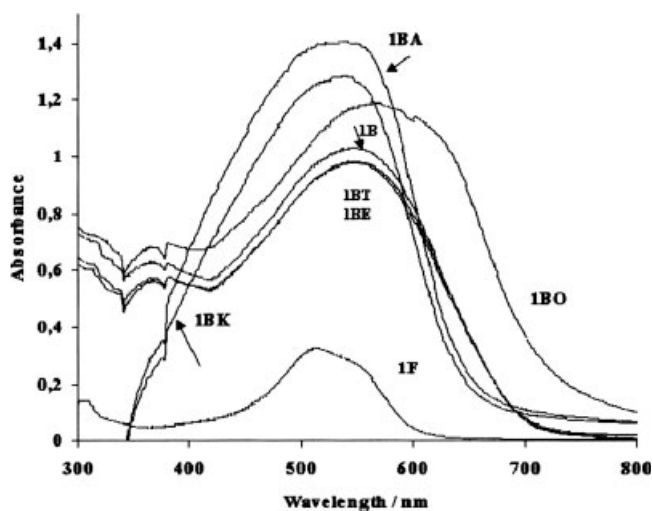


Figure 6 UV–visible spectra of: 1F, model direct dye 1 (aqueous dye solution); 1B, cotton cellulose dyed with dye 1; 1BO, cotton dyed with dye 1 and treated with old sweat (pH = 9.0); 1BT, cotton dyed with dye 1 and treated with thermal sweat (pH = 8.0); 1BE, cotton dyed with dye 1 and treated with effort sweat (pH = 6.5); 1BK, cotton dyed with dye 1 and treated with acidic sweat (pH = 5.5); 1BA, cotton dyed with dye 1 and treated with alkaline sweat (pH = 8.0).

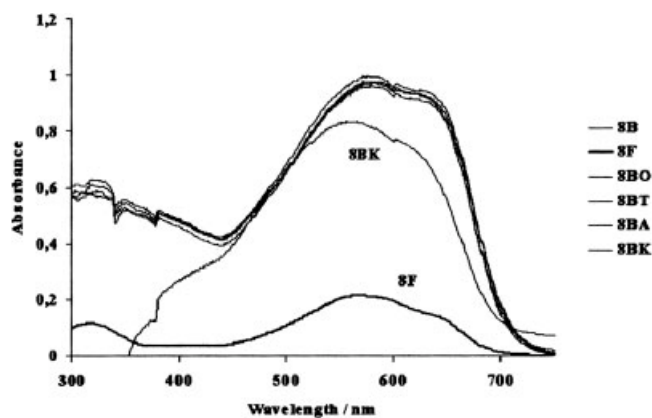


Figure 7 UV–visible spectra of: 8F, model direct dye 8 (aqueous dye solution); 8B, cotton cellulose dyed with dye 8; 8BO, cotton dyed with dye 8 and treated with old sweat (pH = 9.0); 8BT, cotton dyed with dye 8 and treated with thermal sweat (pH = 8.0); 8BE, cotton dyed with dye 8 and treated with effort sweat (pH = 6.5); 8BK, cotton dyed with dye 8 and treated with acidic sweat (pH = 5.5); 8BA, cotton dyed with dye 8 and treated with alkaline sweat (pH = 8.0).

enon, which has been examined for years but still remains not fully understood.

The author thanks Prof. I. Wawer and Dr. Katarzyna Paradowska for the possibility of NMR analysis in Medical University of Warsaw.

References

- Lewin, M.; Pearce, E. M. *Handbook of Fiber Chemistry*; Marcel Dekker: New York, 1998.
- Bikales, N. S.; Segal, L., Eds. *Cellulose and Cellulose Derivatives, Part 5: High Polymers*; Wiley-Interscience: London, 1971.
- Atalla, R. H.; VanderHart, D. L. *Science* 1984, 223, 283.
- VanderHart, D. L.; Atalla, R. H. *Macromolecules* 1984, 17, 1465.
- VanderHart, D. L.; Atalla, R. H. *ACS Symp Ser* 1987, 340, 88.
- Atalla, R. H.; Gast, J. C.; Sindorf, D. W.; Bartuska, V.; Maciel, G. E. *J Am Chem Soc* 1980, 102, 3249.
- Radloff, D.; Boeffel, C.; Spiess, H. W. *Macromolecules* 1996, 29, 1528.
- Sun, X. F.; Sun, R.; Sun, J. X. *J Agric Food Chem* 2002, 50, 6428.
- Love, G. D.; Snape, C. E.; Jarvis, M. C. *Phytochemistry* 1998, 49, 1191.
- Adebajo, M. O.; Frost, R. *Spectrochim Acta Part A* 2004, 60, 449.
- Viscardi, G.; Quagliotto, P.; Barolo, C.; Caputo, G.; Digilio, G.; Degani, I.; Barni, E. *Dyes Pigments* 2003, 57, 87.
- Wiench, J. W.; Schilf, W.; Stefaniak, L.; Webb, G. A. *J Mol Struct* 1999, 510, 1.
- Voss, G. *J Soc Dyers Colourists* 2000, 116, 87.
- Lyčka, A.; Luštinec, D.; Holeček, J.; Nádvořník, M.; Holčápek, M. *Dyes Pigments* 2001, 50, 203.
- Abbott, L. C.; Batchelor, S. N.; Jansen, L.; Oakes, J.; Lindsay Smith, J. R.; Moore, J. N. *New J Chem* 2004, 28, 815.
- Hirai, A.; Horii, F.; Kitamaru, R. *J Polym Sci Polym Phys Ed* 1980, 18, 1801.

17. Colletti, R. F.; Mathias, L. J. *J Appl Polym Sci* 1988, 35, 2069.
18. Princi, E.; Vicini, S.; Pedemonte, E.; Proietti, N.; Capitani, D.; Segre, A. L.; D'Orazio, L.; Gentile, G.; Polcaro, C.; Martuscelli, E. *Macromol Symp* 2004, 218, 343.
19. Chanzy, H.; Henrissat, B.; Vincendon, M.; Tanner, S. T.; Belton, P. S. *Carbohydr Res* 1987, 160, 1.
20. Larsson, P. T.; Westermark, U.; Iversen, T. *Carbohydr Res* 1995, 278, 339.
21. Dudley, R. L.; Fyfe, C. A.; Stephenson, P. J.; Deslandes, Y.; Hamer, G. H.; Marchessault, R. H. *J Am Chem Soc* 1983, 105, 2469.
22. Lennholm, H.; Larsson, T.; Iversen, T. *Carbohydr Res* 1994, 261, 119.
23. Abbott, L. C.; Batchelor, S. N.; Oakes, J.; Lindsay Smith, J. R.; Moore, J. N. *J Phys Chem B* 2004, 108, 13726.
24. Batchelor, S. N.; Oakes, J. *J Phys Org Chem* 2005, 18, 1.
25. Abbott, L. C.; Batchelor, S. N.; Oakes, J.; Gilbert, B. C.; Whitwood, A. C.; Lindsay Smith, J. R.; Moore, J. N. *J Phys Chem A* 2005, 109, 2894.
26. Abbott, L. C.; MacFaul, Ph.; Jjansen, L.; Oakes, J.; Lindsay Smith, J. R.; Moore, J. N. *Dyes Pigments* 2001, 48, 49.
27. Abbott, L. C.; Batchelor, S. N.; Oakes, J.; Lindsay Smith, J. R.; Moore, J. N. *J Phys Chem B* 2004, 108, 10208.
28. Yamaki, S. B.; Barros, D. S.; Garcia, C. M.; Socoloski, P.; Oliveira, O. N., Jr.; Atvars, T. D. *Z. Langmuir* 2005, 21, 5414.
29. Bae, J. S.; Freeman, H. S. *AATCC Rev* 2001, 1, 67.
30. Gudewill, S. *Textilveredlung* 1988, 23, 265.
31. Murakamei, K. *Dyes Pigments* 2002, 53, 31.
32. Shore, J., Ed. *Cellulosics Dyeing*; Society of Dyers and Colourists: Manchester, UK, 1995.
33. Krässig, H. A. *Cellulose*; Gordon Breach Science Publishers: Amsterdam, 1993.
34. Frantz, S.; Hübner, G. A.; Wendland, O.; Roduner, E.; Mariani, C.; Ottaviani, M. F.; Batchelor, S. N. *J Phys Chem* 2005, 109, 11572.
35. Schüürmann, G.; Funar-Timofei, S. *J Chem Inf Comput Sci* 2003, 43, 1502.
36. Pielesz, A.; Paluch, J.; Włochowicz, A. *Adv Colour Sci Technol* 2004, 7, 95.
37. Atalla, R. H.; VanderHart, D. L. *Solid State Nucl Magn Reson* 1999, 15, 1.
38. Sakellariou, D.; Brown, S. P.; Lesage, A.; Hediger, S.; Bardet, M.; Meriles, C. A.; Pines, A.; Emsley, L. *J Am Chem Soc* 2003, 125, 4376.
39. Lasage, A.; Bardet, M.; Emsley, L. *J Am Chem Soc* 1999, 121, 1097.
40. Komo, H.; Yunoki, S.; Shikano, T.; Fujiwara, M.; Erata, T.; Takai, M. *J Am Chem Soc* 2002, 124, 7506.
41. Bardet, M.; Emsley, L.; Vincendon, M. *Solid State Nucl Magn Res* 1997, 8, 25.
42. Koch, F. T.; Preiss, W.; Witter, R.; Sternberg, U. *Macromol Chem Phys* 2000, 201, 1930.
43. Wilson, P. J.; Durran, D. M.; Howlin, B. J.; Webb, G. A. *Electron J Theor Chem* 1996, 1, 18.
44. Viëtor, R. J.; Newman, R. H.; Ha, M. A.; Apperley, D. C.; Jarvis, M. C. *Plant J* 2002, 30, 721.
45. Lyčka, A.; Vrba, Z.; Vrba, M. *Dyes Pigments* 2000, 47, 45.
46. Cross, W. I.; Flower, K. R.; Pritchard, R. G. *J. Chem Res Synop* 1999, 178.
47. Pielesz, A.; Freeman, H. S.; Wysocki, M.; Weselucha-Birczyńska, A.; Włochowicz, A. *Adv Colour Sci Technol* 2003, 6, 4.
48. Pielesz, A.; Weselucha-Birczyńska, A.; Freeman, H. S.; Włochowicz, A. *Cellulose* 2005, 12, 497.
49. Sugiyama, J.; Vuong, R.; Chanzy, H. *Macromolecules* 1991, 24, 2461.
50. Sugiyama, J.; Vuong, R.; Chanzy, H. *Macromolecules* 1991, 24, 4168.
51. Yamamoto, H.; Horii, F. *Macromolecules* 1993, 26, 1313.